The effect of surface roughness on corrosion resistance of machined and epoxy coated steel

C.M.H.Hagen (a), A.Hognestad [1](a), O.Ø.Knudsen (b), K.Sørby (a)

a Department of Mechanical and Industrial Engineering, NTNU, 7491 Trondheim, Norway

b SINTEF, Richard Birkelandsvei 2B, 7465 Trondheim, Norway

Corresponding author: Hagen. E-mail: catalina.hagen@ntnu.no

Abstract

By incorporating periodic micro-patterns on steel substrates, the effect of surface roughness on corrosion resistance of a two-component polyamine cured epoxy mastic coating has been studied. Machining was employed to pattern the surfaces with periodic peaks of varying peak-to-valley heights, Rz. The focus of the study was to find the surface parameter that contributes most to the stability of an organic coating in corrosive environment, and to evaluate if machining can be comparable to blast cleaning with respect to coating durability. A strong correlation between roughness (Rz) and corrosive delamination of coated surfaces was seen. Increasing Rz from 57 µm to 252 µm on surfaces with triangular peaks, increased the effective contact area by 40% and decreased delamination by 30%. By introducing tilted asperities at Rz=224 µm while keeping the effective contact area in general unchanged, delamination decreased another 55%. Hence, an increased Rz is found to be only partially beneficial, and the profile shape is more significant than the roughness value per se. The results suggest that mechanical interlocking has a substantial influence on the interfacial stability of protective coatings in corrosive environments. By optimal selection of cutting parameters, machining can give surfaces where protective coatings have long lifetime.

Highlights

- Triangular shaped peaks with roughness Rz = 252 µm gave a corrosive delamination comparable to that on grit blasted surfaces with Rz = 30-40 µm
- Introducing rectangular peaks with inclination while the effective contact area remained unchanged resulted in a significantly improved corrosion resistance
- Two different delamination behaviors were seen in this study: corrosion creep following a cathodic disbonding front on surfaces patterned with triangular peaks, and corrosion creep alone, at much lower rates, on grit blasted surfaces and surfaces with rectangular tilted peaks.

Keywords: Organic coatings, cathodic disbonding, underfilm corrosion, steel.

[1] Present affiliation: SINTEF Raufoss Manufacturing, Norway

1 Introduction

The most commonly used method for protecting atmospherically exposed steel against corrosion, is the application of protective organic coating systems [1, 2]. It is widely recognized that the stability of the coating-substrate interface is related to the interfacial adhesion forces [2-10] and electrochemical properties [1, 2, 11-16] of this region. The relevance of surface roughness to adhesion has been long recognized [9, 17, 18]. Already in the classical paper from 1925, "On adhesives and adhesive action", McBain and Hopkins considered the roughness of a surface to contribute to adhesion by mechanical interlocking [19]. Brockman suggested bond durability to be determined by the surface roughness, as mechanical interlocking continues to operate even when chemical bonds fail e.g. due to hydrolysis [6].

Several standards describe the characteristics of surfaces to be painted [20-22]. The performance of protective coatings applied to steel are significantly affected by the state of the steel surface prior to painting. Blast cleaning is recommended as pretreatment for most protective coatings in aggressive environments [23, 24]. Nevertheless, for various reasons coatings sometimes must be applied on smooth steel surfaces. Coatings applied on these surfaces are generally found to degrade early with subsequent corrosion of the steel substrate [25].

Studies show in general decreased cathodic disbonding with increased surface profile height [26-28] or with increased interfacial contact area along the profile (tortuosity) [29]. Cathodic disbonding has been found to advance faster along the direction of the surface texture than perpendicular to the surface texture. [27]. In accelerated corrosion tests, Ward found much higher levels of corrosion creep on shot peened samples compared to samples that were grit blasted [30]. The surfaces had comparable profile heights, but rounded versus sharp topographical features, respectively [30]. The effect was by Ward attributed to mechanical interlocking, but could have been explained by tortuosity as well. Adhesion tests have showed that a certain roughness is needed in order to achieve good adhesion [6, 31-33]. A preliminary study to this work showed both weaker adhesion and less corrosion resistance for coatings applied on smooth surfaces compared to grit blasted surfaces [34].

Substantial research has been performed on the effect of various surface parameters on coatings and coating performance, but most of these studies have been performed on surfaces either grit blasted or abraded with grit papers. The topography on such surfaces is a random distribution of irregular grooves and peaks. Hence, it is difficult to investigate how the morphological changes of the surface may influence the corrosion resistance in such studies.

In practice, grit blasting is sometimes not feasible for roughening of a surface, due to functional requirements, logistical or economic reasons. It is therefore important to understand the effect of surface topography on corrosion resistance, and if it is possible to reproduce this effect by other methods than blast cleaning. Hence, in the present study roughness is created by incorporating periodic micro-patterns on steel substrates. Machining is chosen as the surface structuring method, as it is a manufacturing technology heavily implemented in industry for removal of material. Steel components utilized in structural as well as non-structural applications, often

undergo machining before being coated. The focus of the study is to develop a surface texture that improves the stability of an organic coating in corrosive environment. The novelty of the research presented here lies within the use of machining as a method of steel surface preparation, and the combination of machining parameters to create surfaces comparable to grit blasting with respect to coating durability. The goal is to evaluate if machining can be employed to create a surface with equivalent properties to those obtained by grit blasting, with respect to coating stability in corrosive environments.

Through a combination of the machining parameters nose radius, depth of cut, rotational speed and feed, the peak-to-valley height, Rz, of the machined surfaces, was increased. See Table 1 for definition of the roughness parameters used in this study. A periodic pattern of peaks, triangular or rectangular and tilted in profile, was machined into steel surfaces. The surfaces, which were subsequently covered with a commercial two-component polyamine cured epoxy mastic coating, were tested in accelerated corrosion tests and results are correlated with topography (roughness, effective area and morphology). Contact angle measurements were performed to estimate the effect roughness may have on the wetting properties induced by each treatment.

Table 1. Nomenclature. Roughness parameters according to ISO 4287[35] and ISO 4288 [36].

Parameter	Description	Mathematical definition	Typical units
A	Actual surface profile area. The effective contact area.		mm²
A_0	Geometrical area		mm²
L	Actual surface profile length		mm
L_0	Geometrical length		mm
Pc	Peak density.	The number of peaks higher than a certain pre-defined dead-band, e.g. 10% of Rz	Peaks/cm
r	Wenzel's roughness factor	$r=A/A_0$	
Ra	Arithmetic roughness average	$Ra=\frac{1}{l}\sum_{0}^{l}\lvert y\rvert$ l is the measurement length and y the distance from the average line.	µm
Rz	Average maximum peak to valley distance for five sampling lengths within the measurement length l	$Rz=\frac{1}{5}\sum_{i=1}^{5}(Rp+Rv)_i$ Rp is the largest profile peak height and Rv the maximum profile valley depth within one of the five sampling lengths of the measurement length l.	µm
τ	Tortuosity	$\tau=L/L_0$	

2 Experimental

2.1 Steel and surface preparation

The samples were prepared using 5 mm thick plates of structural steel S355J2G3 often used for shipbuilding applications. The chemical composition was 0.14-0.22% C, 0.36-

0.55% Si, 1.23-1.60% Mn, 0.014-0.025% P, 0.029-0.035% S, 0.20 Cr, 0.22 Ni, 0.04 Mo, 0.06% V, 0.27-0.30% Cu, Fe to balance.

Surfaces were machined in CNC machines (computer numerically controlled), by face milling or face turning, see Table 2 for parameters. The parameters were chosen with the intention of creating surfaces with a variation of Rz values, and comparable to the ones found on surfaces after grit blasting. The diameter of the milling cutter was 80 mm. The feed in the milling operation was in the range 0.35-0.73 mm/tooth, and in the range 0.15-0.75 mm/rev in the turning operation.

Surfaces blast cleaned with aluminium oxide (Al_2O_3) were used as reference.

The backside of all samples was grit blasted and edges were rounded.

All machined specimens were degreased with an alkaline degreasing agent, thoroughly rinsed with distilled water and ethanol and dried in an oven at 40 °C. Grit blasted samples were washed with ethanol and dried with an air blower. All samples were placed in a desiccator after preparation until painting.

Table 2. Machining parameters with the resulting roughness, Rz, of the surface. (The values in the parenthesis are standard deviations)

Process	Surface	Nose radius [mm]	Depth of cut [mm]	Feed [mm/tooth]	Feed [mm/rev]	Cutting speed [m/min]	Rz [µm]
Face Milling	M1	0.2	1	0.73	-	25	227 (27)
	M2	0.2	1	0.5	-	25	191 (14)
	M3	0.2	1	0.35	-	25	125 (10)
Face Turning	T1	0.2	0.5	-	0.75	100	675 (9)
	T2	0.2	0.35	-	0.65	100	469 (11)
	T3	0.2	0.3	-	0.5	100	379 (32)
	T4	0.2	0.3	-	0.3	100	62 (2)
	T5	0.2	0.3	-	0.2	100	26 (2)
	T6	0.2	0.3	-	0.1	100	8 (2)
	T7	0.4	0.3	-	0.15	100	11 (3)

2.2 Surface characterization

For surfaces with Rz<100, roughness (Rz) and peak density (Pc) were measured with a stylus profilometer according to ISO 4288 [36], while tortuosity (τ) was measured by a non-contact Alicona optical Infinite-Focus Microscope (IFM). In accordance with Watts [26], the ratio of the actual length measured along the surface profile to the geometrical length, will represent the roughness grade of the cross sectional 2D profile.

For surfaces with Rz>100, roughness (as maximum peak-to-valley distance corresponding to the Rz measured with profilometer), Pc and τ were calculated from cross sections analysed in an Olympus GX51 optical microscope and the IFM. Cross sections were embedded in epoxy, ground with emery papers and polished down to mirror-like surface finish.

Wenzel`s roughness factor (r) was measured with the IFM for all surfaces. The profile parameter was proposed by Wenzel [37], who derived the ratio of the effective contact area divided by the projected geometric area. An increased Wenzel's ratio indicates a higher roughness of the 3D profile and a larger effective contact area at the coating-steel interface.

The morphology of the surfaces was characterized using the 3D-imaging capability of the IFM. Rz values measured by profilometer were confirmed by IFM 3D-imaging measurements.

To analyze the roughness and topography data, the Spearman's correlation coefficient (ρ) was calculated using data analysis software. This coefficient is less sensitive to outliers and shows a low variability.[38-40] The coefficient does not measure the causal relationship between variables, but is used for analyzing correlations. It was assumed that parameters were correlated when the absolute value of the correlation coefficient was greater than 0.7.

As surface roughness/topography affects the wetting properties of surfaces - "the extent to which, at equilibrium, a liquid adhesive will come into contact with a solid surface" [9] - contact angle measurements were conducted to analyze if the corrosion resistance found was influenced by this effect. Static contact angle was measured with a computerized contact angle analyzer (CAM 200, KSV, Finland). A water droplet (MQ-water) was delivered onto the sample surface with a Hamilton syringe mounted on the sample stage. A camera was used to capture side view images of the droplet profile. The contact angle was next calculated by fitting the Young-Laplace equation [41] to the droplet profile. Contact angles were measured in at least two positions for every sample.

2.3 Coating

A commercial two-component polyamine cured epoxy mastic coating was applied on all samples. The coating is specially designed for areas where optimum surface preparation is not possible or desired, and can be used as primer, mid coat or finish coat in atmospheric and immersed environments. The volume fraction of solids was 82%. In this study, the corrosion resistance was studied on samples having at least two layers with total dry film thickness (TDFT) measured to 350-400 µm. On milled surfaces, the coating was applied by an adjustable film applicator, while turned surfaces were spray coated. Each coat was allowed to cure for one day before application of next coat. The coatings were finally baked for two days at 40 °C. The backside and the edges of the samples were sealed with the same epoxy mastic coating.

2.4 Accelerated corrosion test

An accelerated corrosion test was performed according to ISO 12944-9, except that the samples were only exposed in 6-8 test cycles instead of 25 [42]. This is a cyclic wet/dry corrosion test, widely used for testing the performance of marine and offshore coatings and found to have a certain correlation to field performance [43, 44], see Table 3.

Table 3: Description of ISO 12944-9 test cycle.

Day 1	Day 2	Day 3	Day 4	Day 5	Day 6	Day 7
4h UVA 60°C / 4h Condensation 50°C			Salt spray NaCl 5% 35°C			-20°C

A 50 mm long and 2 mm wide scribe was machined down to the steel substrate prior to testing, to initiate corrosion perpendicular to the surface texture. The test evaluates the resistance against corrosion creep. Cathodic disbonding was found in front of the corrosion creep on many of the machined surfaces. Corrosion creep and cathodic disbonding was measured at 9 different positions along the 50 mm scribe, according to ISO 15711[45]. At least three replicate panels for each surface treatment were tested.

3 Results and discussion

3.1 Surface characterization

In machining operations, the surface roughness increases rapidly with the increase in feed rate [46, 47]. By face turning and milling at variable feed rates, two types of periodic surface profiles were produced: 1) surfaces with a periodic distribution of peaks triangular in profile and 2) surfaces with a periodic distribution of rectangular, tilted peaks. Figure 1 shows images of cross-sections and surface area representing the two profiles, along with a grit blasted surface.

The roughness Rz on surfaces patterned with periodic triangular peaks was measured to be in the range 7–252 µm. Surfaces patterned with periodic rectangular, tilted peaks was in the range 224–683 µm. The inclination of the peaks was measured to be in the range 50-180 µm. The inclination was measured as the longest distance between the peak and the normal to the peak, as illustrated by the arrow in the lower image of Figure 1.

Grit blasting generated surfaces with a random distribution of irregular cavities and coarse morphologies with undercuts. Surfaces with Rz between 27 to 48 µm were obtained and used as reference.

There are several available standards with recommendations regarding the pre-treatment of steel surfaces to be coated. Selection of protective coatings for offshore installations and associated facilities can follow NORSOK M-501 [24] or ISO 12944 [23]. Both recommend blast cleaning that complies with ISO 8501-1 Sa 2½, which is a cleanliness recommendation. The roughness is stated to be in accordance with the

requirements for the coating system chosen and correspond to a roughness Rz 50-115 µm. Considering these recommendations, the roughness grades of the machined surfaces were well beyond the requirements, while blast cleaned surfaces had lower roughness. The surfaces were however fitted for the epoxy employed.

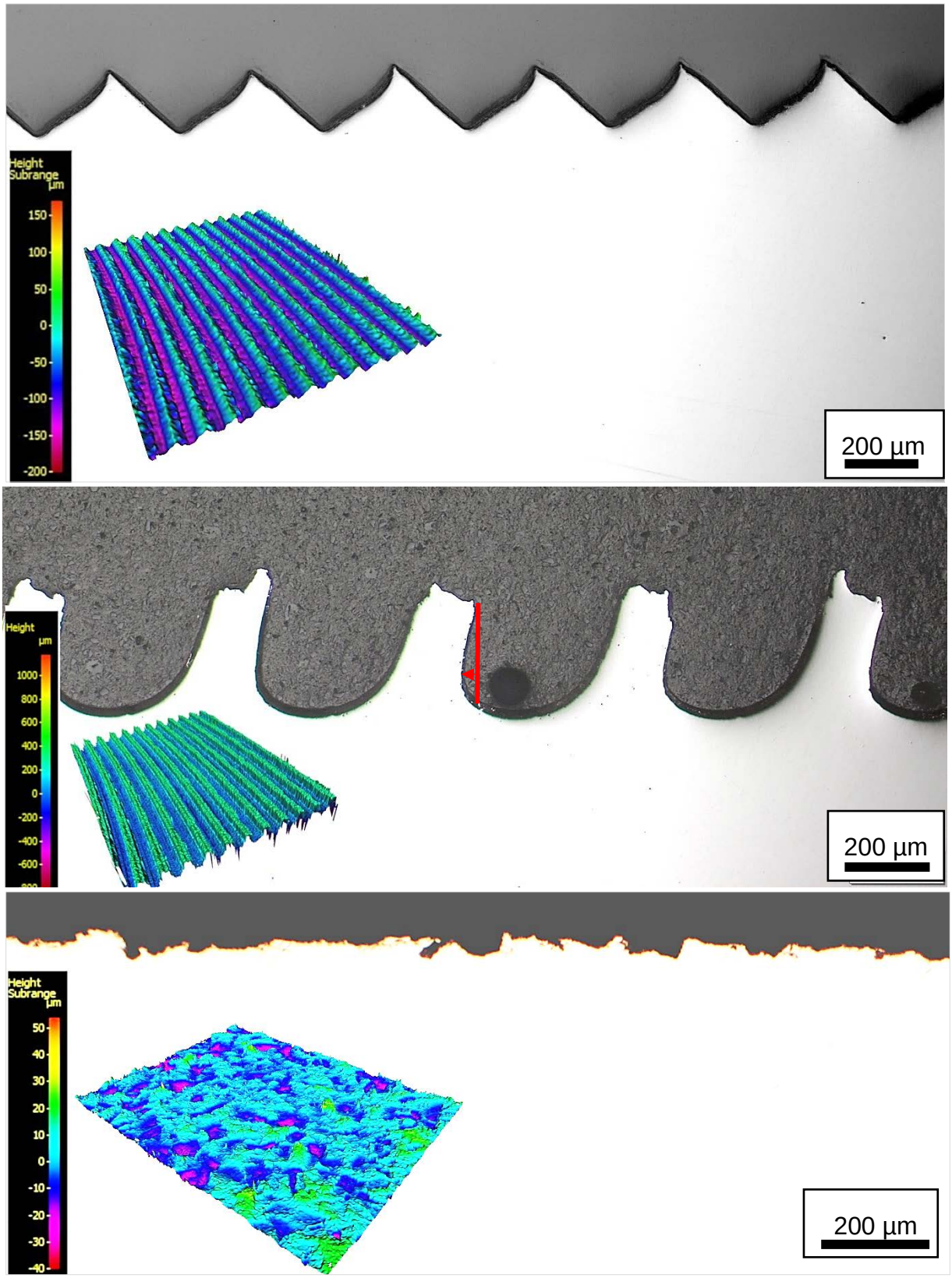

Figure 1. Optical microscope images, in black and white, of cross sections of surfaces machined with triangular peaks (upper), rectangular and tilted peaks (center), and grit blasted surfaces (lower). 3D images of surface area scanned by focus-variation with IFM, seen in colors indicating the level of roughness.

Wenzel's roughness factor increased linearly with Rz. The relationship was confirmed with a high significance for the periodic ($r=0.96$, $p<0.01$) and grit blasted surfaces ($r=0.922$, $p<0.01$), indicating a strong positive correlation between the effective contact area at the coating-substrate interface and the peak-to-valley height. The increase in effective contact area can potentially provide a larger interface for bonding of the applicable organic coating [9, 48].

Grit blasted surfaces had Wenzel's roughness factors from 1.2 to 1.3. Sørensen found the ratio of actual length to geometrical length to be 1.15 and 1.18 on grit blasted steel with surface roughness values, Rz=52 µm and Rz= 41.6 µm respectively[29], hence measurements correlate well with earlier findings. See Figure 2 for information about the relationship between the roughness Rz and the effective contact area defined by Wenzel's roughness factor. Surfaces with periodic triangular peaks had Wenzel's roughness factors from 1.1 to 1.9. Surfaces with periodic rectangular tilted peaks had Wenzel's roughness factor from 2 to 4.3.

Figure 2. The relationship between roughness Rz, and Wenzel's roughness factor (effective contact area).

Figure 2 shows that machined surfaces with triangular peaks at Rz<100 μm and grit blasted surfaces had similar Wenzel's roughness factor at comparable Rz roughness values.

It was wished to estimate the effect roughness may have on the wetting properties induced by each treatment. In Figure 3 average values for apparent contact angles are reported for the surfaces in this study. On non-ideal surfaces, e.g. rough, non-porous or heterogenous surfaces, contact angle measurements are quite challenging and frequently produce unreliable results [49, 50]. On such surfaces, the only measurable value is the apparent contact angle.

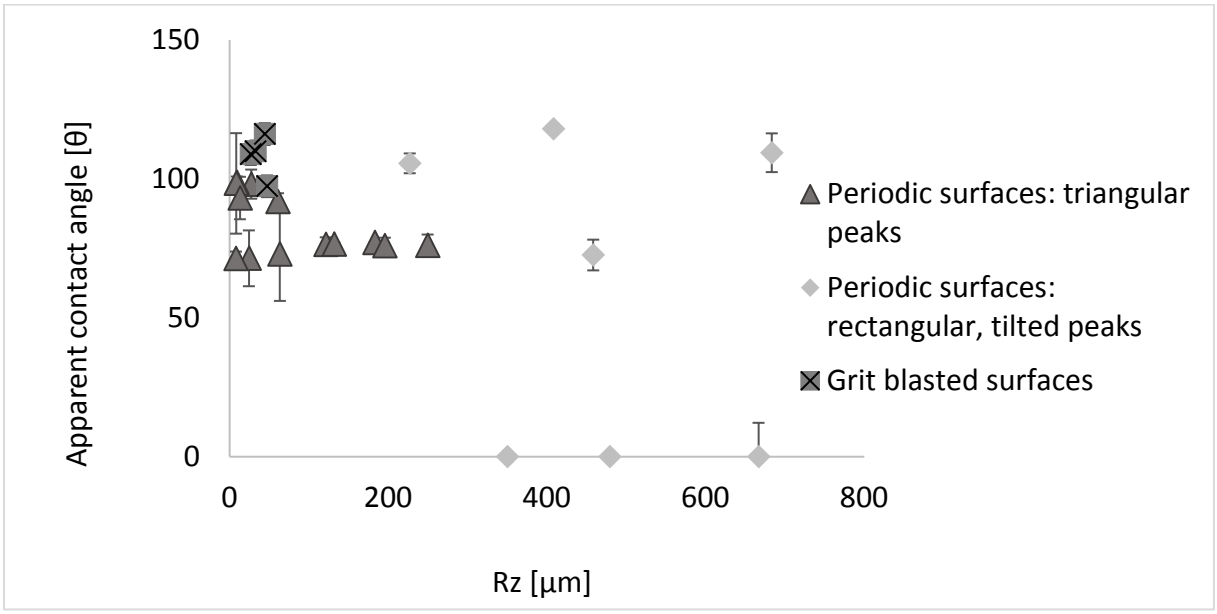

Figure 3. The relationship between contact angle values - on surfaces patterned with periodic triangular peaks and rectangular and tilted peaks - and roughness Rz. Grit blasted surfaces for comparison.

On rough surfaces the apparent contact angle will however be affected by the droplet volume and may also change from point to point along the contact line between the water droplet and the substrate. Measuring and calculating an average value of the apparent contact angle over several droplets is advised in order to overcome the latter problem [51]. For surfaces with triangular peaks, apparent contact angles were between 71° and 98°. For rectangular peaks these were between 0° and 118°, while for grit blasted surfaces these were found to be between 97° and 116°.

Apparent contact angles correlated well with previous findings. On mild steel treated to have different types of oxides, it has been measured water contact angles between 20° and 75° [52]. On mild steel surfaces prepared with a range of techniques like water-jetting and abrasive blasting, the measured contact angle was between 62.8° and 114.2° [33]. Contact angles were seen to increase with the effective contact area. To examine the wettability of the surfaces, it is necessary to correct for the effect of the surface profile on the measured apparent contact angles. The Wenzel's roughness

factor was derived for this purpose, who stated that adding roughness to a surface would amplify the wetting properties of a given surface, by influencing the intrinsic contact angle according to the equation Eq.(1)

$$\cos\theta_{\text{apparent}} = r \times \cos\theta_{\text{intrinsic}} \quad (1)$$

There was no indication of differences in wetting properties for the different surfaces, as no relationship was found between delamination rates and Wenzel corrected contact angles measured on bare surfaces, see Figure 4.

It is worth to highlight that one main implication of Wenzel's equation, is that roughness makes hydrophilic surfaces $(\theta_{\text{intrinsic}} < 90^{\circ})$ more hydrophilic and hydrophobic surfaces $(\theta_{\text{intrinsic}} > 90^{\circ})$ more hydrophobic. This is in general not in accordance with the results presented here, which indicate increased hydrophobicity on surfaces with rectangular peaks or irregular profile (grit blasted surfaces). Several workers have also observed that roughening a substrate usually causes its wettability to decrease [31, 33, 53], and a number of hypotheses have been proposed to explain the wetting properties of smooth and rough surfaces. The authors explained the findings as most likely caused by the topography, and Herminghaus has shown that by creating overhanging intendations on initially hydrophilic surfaces, these will behave hydrophobically [54]. This liquid-repellent property will not be an equilibrium property. His findings resemble our own experience, as the droplet of liquid placed on surfaces grit blasted or patterned with rectangular, tilted peaks, spread out after 9-20 seconds and resulted in complete wetting of the surface.

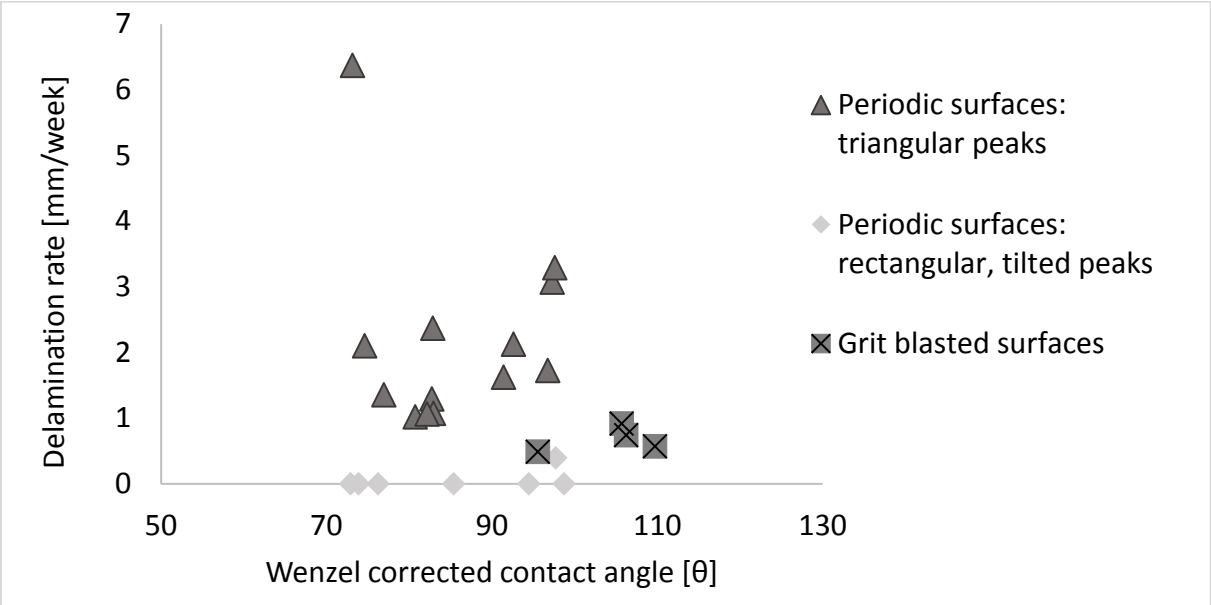

Figure 4. The effect of roughness on wettability and delamination rate. Delamination rate as a function of Wenzel corrected contact angles, hence angles corrected for the effect of roughness, for the surfaces employed in this study.

3.2 Delamination

In general, two different delamination behaviors were seen in this study: corrosion creep following a cathodic disbonding front, and corrosion creep alone (at much lower rates).

On surfaces machined with triangular peaks, delamination was found to happen as a combination of corrosion creep and cathodic disbonding, see Figure 5. The cathodic disbonding was identified as a non-corroded area ahead of the corrosion creep with delaminated coating. The pH at this location was measured with pH indicator strips to be above 10. This is representative for cathodic disbonding, caused by reduction of oxygen beneath the paint.

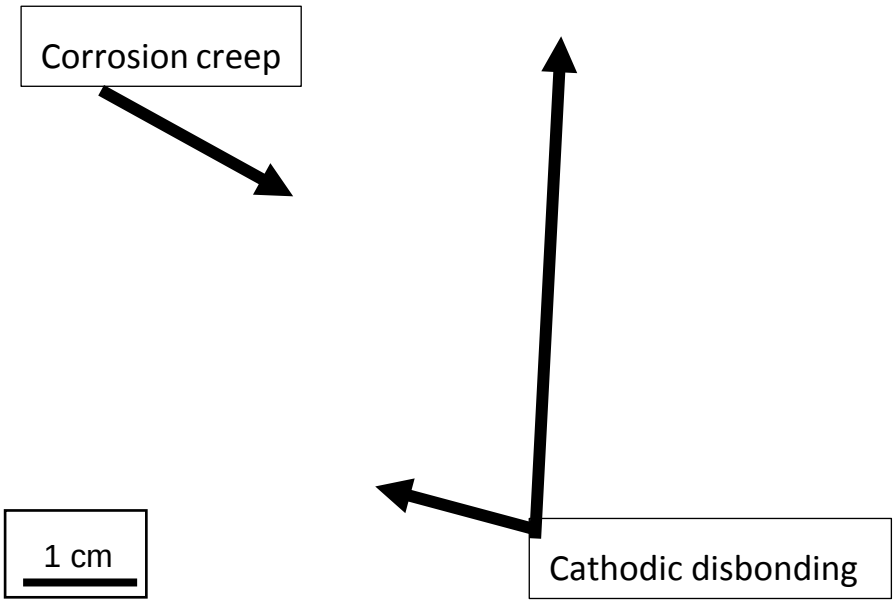

Figure 5. The delaminated area, containing a zone covered with corrosion products, identified as corrosion creep and an area area ahead of the corrosion creep, with delaminated coating but no corrosion products present on the surface, identified as cathodic disbonding.

Delamination rates were calculated as the sum of the corrosion creep and cathodic disbonding and divided by the time the test lasted [55]. Delamination rates were seen to decrease with increased Rz, see Figure 6. Results from delamination tests have not been averaged but are presented for all 76 tests (15 grit blasted and 61 machined surfaces).

It was found that at comparable roughness and effective contact area, delamination was two-three times higher for surfaces machined with triangular peaks than for grit blasted surfaces. A six-seven times increase in Rz was needed for machined surfaces with periodic triangular peaks to give similar delamination rate values as found for grit blasted surfaces at comparable roughness and effective contact area. For example, grit blasted surfaces with Rz = 33 µm, were found to have a delamination rate of 0.74 mm/week. The triangular peaks had comparable delamination rates at Rz > 212 µm.

No delamination was found on surfaces with rectangular, tilted peaks with Rz>350 µm after 8 test cycles. For these surfaces, the cyclic testing was therefore prolonged to a total of 30 cycles. The delamination rates seen in Figure 6 for these samples, are hence calculated from the delamination found after the 30 test cycles.

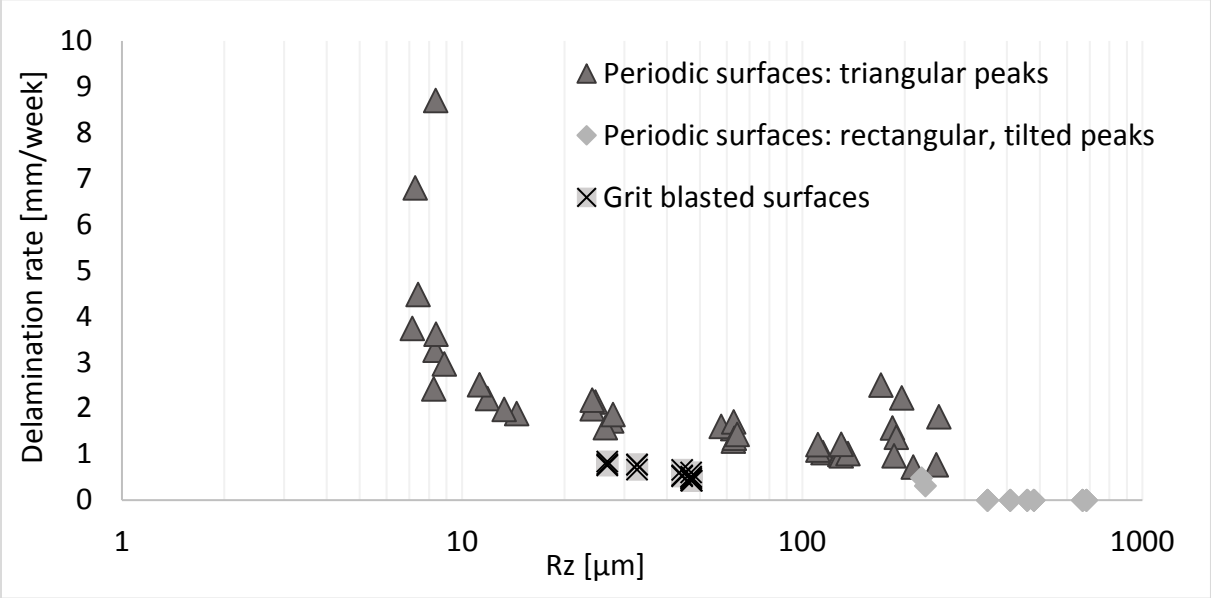

Figure 6. Semi-log plot of delamination rate as function of surface roughness, Rz. The scale on the x-axis is logarithmic.

The contrast in corrosion resistance between the surfaces with triangular peaks and surfaces with rectangular and tilted peaks is noteworthy to highlight: The delamination – sum of corrosion creep and cathodic disbonding – after 8 weeks of testing, was found to be 8.84 mm on the average on surfaces with triangular peaks having Rz values between 212 µm and 252 µm. On the surfaces with rectangular, tilted peaks at Rz=224-230 µm, the delamination – measured solely as corrosion creep – was measured to be 3.2 mm on the average after 8 weeks of testing. After 30 weeks of testing, the delamination – measured solely as corrosion creep – was measured to 1.71 mm on the average on surfaces with rectangular tilted peaks with Rz=350 µm. No grit blasted surfaces at such high Rz values were tested, but the delamination – measured solely as corrosion creep – on grit blasted surfaces with Rz=47 µm, was measured to 3.9 mm after 8 weeks of testing. Hence at the same level as found on surfaces with rectangular, tilted peaks at Rz=224-230 µm. As the effective contact area was found to increase with increase Rz, as seen in Figure 2, the effective contact area was comparable at comparable Rz values on the surfaces with triangular peaks and grit blasted surfaces. Similarly, for surfaces with triangular peaks and rectangular tilted peaks the effective contact area was comparable at comparable roughness Rz.

The humid environment is probably the main determinant on the durability of the coating-metal bond. During exposure to a corrosive environment, several factors contribute to degradation of the coating-steel interface: i) the saturation of the coatings by water lowers coating adhesion [6, 8], ii) the cyclic wet/dry exposure increases the internal stresses in the polymer and lead to microcracking at the coating surface [27],

iii) corrosion products at defects exert stresses on the coating-substrate interface [56, 57], iv) the cathodic reaction underneath the coating will increase the local pH and break the coating-substrate bonds. In humid environments, electrochemical de-adhesion is found to initiate at damage or weaknesses in the coating [2, 58-60] and to propagate by anodic undermining [2, 12, 15], cathodic disbonding [59-64] or oxide wedging [56], depending on the coating system, exposure environment and substrate.

Increasing Rz from 57 µm to 252 µm on surfaces with triangular peaks, increased the effective contact area by 40% and decreased delamination by 30%. By introducing tilted asperities at Rz=224 µm while keeping the effective contact area unchanged, delamination decreased another 55%. Hence, an increased Rz is found to be only partially beneficial, verifying that the surface profile is more significant than the roughness value per se, as previously reported by Ward [30]. Machined surfaces with triangular peaks have poor wet adhesion properties, at least at low roughness values, when compared to grit blasted surfaces [34]. It is assumed that although wet-adhesion properties may improve with increased roughness, a coating/metal interface weakened by exposure to humidity will greatly facilitate corrosive delamination when the surface does not allow for mechanical interlocking [48].

The tilted peaks introduce cavities at the surface, resembling the irregular topography with undercuts found on grit blasted surfaces. The coating adhering within these pockets may result in the improved delamination resistance seen not only on the surfaces with tilted peaks, but also explaining the higher corrosion resistance of coatings on grit blasted surfaces.

The increase in effective contact area is however also important. Interfacial adhesion is known to originate from several contributions: a) physical interactions, b) chemical bonds, c) mechanical interlocking and d) heat dissipation [65, 66]. Both the physical and the chemical interactions are related to the unit area of interface and will be affected by an increase in the effective contact area. The increase will however not only lead to a change in the contribution to interfacial adhesion with respect to a) and b), but also to mechanical interlocking c), where this is possible.

Based on the results presented, it is believed that machining can be employed as pre-treatment to fabricate surfaces that may present similar properties as grit blasted surfaces when it comes to corrosion resistance of a two-component polyamine cured epoxy mastic coating. Roughness values must however be well above 200 µm to show a delamination behaviour comparable to grit blasted surfaces at fine-medium roughness grade, Rz=30-40. It is believed that a certain inclination must be added to the peaks, for surfaces to have the same properties or better as grit blasted have in means of corrosion resistance of a two-component polyamine cured epoxy mastic coating.

4 Conclusions

Face turning and milling of steel at different feeds and depth of cuts resulted in surfaces patterned with peaks of varying size and morphology - triangular and tilted rectangular peaks. The rectangular peaks were however only possible to fabricate at roughness values Rz>224 µm.

Accelerated corrosion tests showed that the corrosive delamination of a two-component polyamine cured epoxy mastic coating from machined surfaces is partially explained by the lower roughness found on these surfaces. Increasing the roughness by means of increased peak-to-valley height, resulted in decreased delamination rate on all surfaces. A linear correlation between the roughness and the effective contact area was found for both grit blasted and machined surfaces. The effective contact area affects the physical and chemical interactions, as these are related to the unit area they are acting over. Hence, the decreased delamination rates found with increased roughness may be related to an increase in effective contact area. However, the lack of cavities on surfaces with triangular peaks eliminates their ability for mechanical interlocking. As long as the surface's ability for mechanical interlocking remains low, the interfacial stability of protective coatings in corrosive environments will need roughness values at least six times higher than needed for grit blasted surfaces. High roughness may hence be a partial substitution for mechanical interlocking.

5 Acknowledgements

Thanks to the Research Council of Norway under contract number 235239 /O70, Brunvoll, Omya Hustadmarmor, Triplex and AquaMarine for financial support of this investigation.

6 Data availability

The raw/processed data required to reproduce these findings cannot be shared at this time as the data also forms part of an ongoing study.

References

1. Stratmann, M., R. Feser, and A. Leng, *Corrosion protection by organic films.* Electrochimica Acta, 1994. **39**(8–9): p. 1207-1214.
2. Grundmeier, G., W. Schmidt, and M. Stratmann, *Corrosion protection by organic coatings: electrochemical mechanism and novel methods of investigation.* Electrochimica Acta, 2000. **45**(15–16): p. 2515-2533.
3. Wielant, J., et al., *Influence of the Iron Oxide Acid−Base Properties on the Chemisorption of Model Epoxy Compounds Studied by XPS.* The Journal of Physical Chemistry C, 2007. **111**(35): p. 13177-13184.
4. Wielant, J., et al., *SKP as a tool to study the physicochemical interaction at buried metal–coating interfaces.* Surface and Interface Analysis, 2010. **42**(6-7): p. 1005-1009.
5. Funke, W., *Toward a unified view of the mechanism responsible for paint defects by metallic corrosion.* Industrial & Engineering Chemistry Product Research and Development, 1985. **24**(3): p. 343-347.
6. Brockmann, W., *Durability of Adhesion Between Metals and Polymers.* The Journal of Adhesion, 1989. **29**(1-4): p. 53-61.
7. Mittal, K.L., *Adhesion measurement: Recent progress, unsolved problems, and prospects*, in *Adhesion measurement of thin films, thick films, and bulk coatings*, K.L. Mittal, Editor 1978, ASTM: Philadelphia, PA.
8. Leidheiser, H. and W. Funke, *Water Disbondment and Wet Adhesion of Organic Coatings on Metals: a Review and Interpretation.* J. Oil Colour Chem. Assoc., 1987. **70**(5): p. 121-132.

9. Packham, D.E., *Surface roughness and adhesion,* in *Adhesion Science and Engineering*, M. Chaudhury and A.V.Pocius, Editors. 2002, Elsevier Science B.V.: Amsterdam. p. 317-349.
10. Nazarov, A. and D. Thierry, *Hydrolysis of interfacial bonds in a metal/polymer electrical double layer.* Protection of metals 2005. **41**(2): p. 105-116.
11. Hausbrand, R., M. Stratmann, and M. Rohwerder, *The Physical Meaning of Electrode Potentials at Metal Surfaces and Polymer/Metal Interfaces: Consequences for Delamination.* Journal of The Electrochemical Society, 2008. **155**(7): p. C369-C379.
12. Posner, R., O. Ozcan, and G. Grundmeier, *Water and Ions at Polymer/Metal Interfaces*, in *Design of Adhesive Joints Under Humid Conditions*, M.L.F. Silva and C. Sato, Editors. 2013, Springer Berlin Heidelberg: Berlin, Heidelberg. p. 21-52.
13. Nazarov, A. and D. Thierry, *Studies in the Electrical Double Layer at Metal/Polymer Interfaces by Scanning Capacitive Probe.* Protection of metals 2003. **39**(1): p. 55-62.
14. Nazarov, A. and D. Thierry, *Mechanism of the Corrosion Exfoliation of a Polymer Coating from Carbon Steel.* Protection of metals 2009. **45**(6): p. 735-745.
15. Nazarov, A. and D. Thierry. *Influence of Electrochemical Conditions in a Defect on the Mode of Paint Corrosion Delamination from a Steel Surface*. in *CORROSION 2010*. 2010.
16. Stratmann, M., *2005 W.R. Whitney Award Lecture: Corrosion stability of Polymer-Coated Metals - New Consepts Based on Fundamental Understanding.* Corrosion, 2005. **61**(12): p. 1115-1126.
17. Packham, D.E., *The mechanical theory of adhesion - a seventy year perspective and its current status*, in *First international congrenss on adhesion science and technology*, W.J.v. Ooij and H.R. Andersen, Editors. 1998, VSP: Utrecht, Netherlands. p. 28 p.
18. Packham, D.E., *Surface energy, surface topography and adhesion.* International Journal of Adhesion and Adhesives, 2003. **23**(6): p. 437-448.
19. McBain, J.W. and D.G. Hopkins, *On Adhesives and Adhesive Action.* The Journal of Physical Chemistry, 1925. **29**(2): p. 188-204.
20. Standardization, I.O.f., *Preparation of steel substrates before application of paints and related products -- Visual assessment of surface cleanliness -- Part 1: Rust grades and preparation grades of uncoated steel substrates and of steel substrates after overall removal of previous coatings*, 2007, International Organization for Standardization: Switzerland.
21. Standardization, I.O.f., *Surface roughness characteristics of blast-cleaned steel substrates -- Part 4: Method for the calibration of ISO surface profile comparators and for the determination of surface profile -- Stylus instrument procedure*, 2012, International Organization for Standardization: Switzerland.
22. Standardization, I.O.f., *Preparation of steel substrates before application of paints and related products -- Surface roughness characteristics of blast-cleaned steel substrates -- Part 2: Method for the grading of surface profile of abrasive blast-cleaned steel -- Comparator method*, 2012, International Organization for Standardization: Switzerland.
23. Standardization, I.O.f., *Paints and varnishes -- Corrosion protection of steel structures by protective paint systems*, 2007, International Organization for Standardization: Switzerland.
24. Norway, S., *Surface preparation and protective coating*, 2012, Standards Norway: Oslo.
25. Knudsen, O., *Review of Coating Failure Incidents on the Norwegian Continental Shelf since the Introduction of NORSOK M-501*, in *CORROSION 2013*, NACE, Editor 2013, NACE

26. Watts, J.F. and J.E. Castle, *The application of X-ray photoelectron spectroscopy to the study of polymer-to-metal adhesion. Part 2 The cathodic disbondment of epoxy coated mild steel.* Journal of Materials Science, 1984. **19**: p. 2259-72.
27. Khun, N.W. and G.S. Frankel, *Effects of surface roughness, texture and polymer degradation on cathodic delamination of epoxy coated steel samples.* Corrosion Science, 2013. **67**: p. 152-160.
28. Ghaffari, M., et al., *Demonstration of epoxy/carbon steel interfacial delamination behavior: Electrochemical impedance and X-ray spectroscopic analyses.* Corrosion Science, 2016. **102**(Supplement C): p. 326-337.
29. Sørensen, P.A., et al., *Influence of substrate topography on cathodic delamination of anticorrosive coatings.* Progress in Organic Coatings, 2009. **64**(2–3): p. 142-149.
30. Ward, D., *An Investigation Into The Effect Of Surface Profile On The Performance Of Coatings In Accelerated Corrosion Tests*, in *CORROSION 2007*2007, NACE: Houston, TX. p. p. 16.
31. Harris, A.F. and A. Beevers, *The effects of grit-blasting on surface properties for adhesion.* International Journal of Adhesion and Adhesives, 1999. **19**(6): p. 445-452.
32. Islam, M.S., L. Tong, and P.J. Falzon, *Influence of metal surface preparation on its surface profile, contact angle, surface energy and adhesion with glass fibre prepreg.* International Journal of Adhesion and Adhesives, 2014. **51**(0): p. 32-41.
33. Jamali, S.S. and D.J. Mills, *Steel surface preparation prior to painting and its impact on protective performance of organic coating.* Progress in Organic Coatings, 2014. **77**(12, Part B): p. 2091-2099.
34. Hagen, C.H.M., A. Kristoffersen, and O.Ø. Knudsen, *The Effect of Surface Profile on Coating Adhesion and Corrosion Resistance*, in *CORROSION 2016*, NACE, Editor 2016, NACE Vancouver. p. p. 15.
35. Standardization, I.O.f., *Geometrical Product Specifications (GPS) - Surface texture: Profile method -Terms, definitions and surface texture parameters*, 2000, International Organization for Standardization: Switzerland.
36. Standardization, I.O.f., *Geometrical Product Specifications (GPS) - Surface texture : Profile method -- Rules and procedures for the assessment of surface texture*, 1996, International Organization for Standardization: Switzerland.
37. Wenzel, R.N., *Resistance of solid surfaces to wetting by water.* Industrial & Engineering Chemistry, 1936. **28**(8): p. 988-994.
38. Hauke, J. and T. Kossowski, *Comparison of values of Pearson's and Spearman's correlation coefficients on the same sets of data.* Quaestiones Geographicae, 2011. **30**(2): p. 87-93.
39. Hryniewicz, O. and J. Karpinski, *Prediction of reliability – the pitfalls of using Pearson's correlation.* Maintenance and Reliability, 2014. **16**(3): p. 472-483.
40. Kim, Y., T.-H. Kim, and T. Ergün, *The instability of the Pearson correlation coefficient in the presence of coincidental outliers.* Finance Research Letters, 2015. **13**: p. 243-257.
41. Hiemenz, P.C. and R. Rajagopalan, *Principles of colloid and surface chemistry*. 3rd ed1997, New York - Basel: CRC Press. 672.
42. Standardization, I.O.f., *Paints and varnishes -- Corrosion protection of steel structures by protective paint systems -- Part 9: Protective paint systems and laboratory performance test methods for offshore and related structures*, 2018, International Organization for Standardization: Switzerland.
43. Le Bozec, N., et al., *Performance of marine and offshore paint systems: Correlation of accelerated corrosion tests and field exposure on operating ships.* Materials and corrosion, 2015. **66**(3): p. 215-225.

44. Le Bozec, N., C. Hall, and D. Melot. *Comparison of accelerated ageing tests as per ISO 20340 Annex A and NACE SP0108 standards*. in *CORROSION 2014*. 2014. San Antonio: NACE International.
45. Standardization, I.O.f., *Paints and varnishes -- Determination of resistance to cathodic disbonding of coatings exposed to sea water*, 2003, International Organization for Standardization: Switzerland.
46. Benardos, P.G. and G.C. Vosniakos, *Predicting surface roughness in machining: a review*. International Journal of Machine Tools and Manufacture, 2003. **43**(8): p. 833-844.
47. Karayel, D., *Prediction and control of surface roughness in CNC lathe using artificial neural network.* Journal of Materials Processing Technology, 2009. **209**(7): p. 3125-3137.
48. Venables, J.D., *Adhesion and durability of metal-polymer bonds.* Journal of Materials Science, 1984. **19**(8): p. 2431-2453.
49. Meiron, T.S., A. Marmur, and I.S. Saguy, *Contact angle measurement on rough surfaces.* Journal of Colloid and Interface Science, 2004. **274**(2): p. 637-644.
50. Chau, T.T., *A review of techniques for measurement of contact angles and their applicability on mineral surfaces.* Minerals Engineering, 2009. **22**(3): p. 213-219.
51. Wolansky, G. and A. Marmur, *Apparent contact angles on rough surfaces: the Wenzel equation revisited.* Colloids and Surfaces A: Physicochemical and Engineering Aspects, 1999. **156**(1): p. 381-388.
52. Wielant, J., et al., *Cathodic delamination of polyurethane films on oxide covered steel – Combined adhesion and interface electrochemical studies.* Corrosion Science, 2009. **51**(8): p. 1664-1670.
53. Rupp, F., et al., *Roughness induced dynamic changes of wettability of acid etched titanium implant modifications.* Biomaterials, 2004. **25**(7): p. 1429-1438.
54. Herminghaus, S., *Roughness-induced non-wetting.* Europhys. Lett., 2000. **52**(2): p. 165-170.
55. Axelsen, S.B. and O. Knudsen, *The effect of water-soluble salt contamination on coating performance*, in *CORROSION 2011*2011, NACE.
56. Kappes, M., G.S. Frankel, and N. Sridhar, *Adhesion and adhesion degradation of a pressure sensitive tape on carbon steel.* Progress in Organic Coatings, 2010. **69**(1): p. 57-62.
57. Tayler, M.L., et al., *Scribe Creep and Underpaint Corrosion on Ultra-High Molecular Weight Epoxy Resin Coated 1018 Steel Part 2: Scribe Creep Model as a Function of Environmental Severity Factors.* Corrosion, 2015. **71**(3): p. 326-342.
58. Montoya, R., et al., *A cathodic delamination study of coatings with and without mechanical defects.* Corrosion Science, 2014. **82**(0): p. 432-436.
59. Fürbeth, W. and M. Stratmann, *The delamination of polymeric coatings from electrogalvanised steel – a mechanistic approach.: Part 1: delamination from a defect with intact zinc layer.* Corrosion Science, 2001. **43**(2): p. 207-227.
60. Fürbeth, W. and M. Stratmann, *The delamination of polymeric coatings from electrogalvanized steel – a mechanistic approach.: Part 2: delamination from a defect down to steel.* Corrosion Science, 2001. **43**(2): p. 229-241.
61. Leng, A., H. Streckel, and M. Stratmann, *The delamination of polymeric coatings from steel. Part 2: First stage of delamination, effect of type and concentration of cations on delamination, chemical analysis of the interface.* Corrosion Science, 1998. **41**(3): p. 579-597.

62. Leng, A., H. Streckel, and M. Stratmann, *The delamination of polymeric coatings from steel. Part 1: Calibration of the Kelvinprobe and basic delamination mechanism.* Corrosion Science, 1998. **41**(3): p. 547-578.
63. Leng, A., et al., *The delamination of polymeric coatings from steel. Part 3: Effect of the oxygen partial pressure on the delamination reaction and current distribution at the metal-polymer interface.* Corrosion Science, 1999. **41**(3): p. 599-620.
64. Fürbeth, W. and M. Stratmann, *The delamination of polymeric coatings from electrogalvanized steel – a mechanistic approach.: Part 3: delamination kinetics and influence of CO2.* Corrosion Science, 2001. **43**(2): p. 243-254.
65. Hölck, O., et al., *Comparative characterization of chip to epoxy interfaces by molecular modeling and contact angle determination.* Microelectronics Reliability, 2012. **52**(7): p. 1285-1290.
66. Sluis, O.v.d., S.P.M. Noijen, and P.H.M. Timmermans, *On the effect of microscopic roughness on macroscopic polymer-metal adhesion*, in *Solid state lighting reliability: components to systems*, W.D.v. Driel and X.J.Fan, Editors. 2013, Springer.